




Modeling the Impact of Climate Extremes on Seasonal Influenza Outbreaks Across Tropical and Temperate Locations

Aleksandra R. Stamper^{1,2} , Ayesha S. Mahmud³, Jennifer R. Nuzzo¹, and Rachel E. Baker^{1,2}

¹Department of Epidemiology, Brown University, Providence, RI, USA, ²Institute at Brown for Environment and Society, Brown University, Providence, RI, USA, ³Department of Demography, University of California, Berkeley, CA, USA

Key Points:

- Patterns of climate variability are expected to increase with climate change, leading to more frequent and severe weather extremes
- Absolute humidity and temperature are known climate drivers of influenza transmission
- Increasing climate variability stands to impact seasonal influenza outbreaks, which can be explored using mechanistic epidemiologic models

Supporting Information:

Supporting Information may be found in the online version of this article.

Correspondence to:

A. R. Stamper,
aleksandra_stamper@brown.edu

Citation:

Stamper, A. R., Mahmud, A. S., Nuzzo, J. R., & Baker, R. E. (2025). Modeling the impact of climate extremes on seasonal influenza outbreaks across tropical and temperate locations. *GeoHealth*, 9, e2024GH001138. <https://doi.org/10.1029/2024GH001138>

Received 21 JUN 2024
 Accepted 30 JAN 2025

Author Contributions:

Conceptualization: Rachel E. Baker
Data curation: Aleksandra R. Stamper, Rachel E. Baker
Formal analysis: Aleksandra R. Stamper
Funding acquisition: Jennifer R. Nuzzo
Methodology: Aleksandra R. Stamper
Resources: Aleksandra R. Stamper
Visualization: Aleksandra R. Stamper
Writing – original draft: Aleksandra R. Stamper
Writing – review & editing: Aleksandra R. Stamper, Ayesha S. Mahmud, Jennifer R. Nuzzo, Rachel E. Baker

© 2025 The Author(s). GeoHealth published by Wiley Periodicals LLC on behalf of American Geophysical Union. This is an open access article under the terms of the [Creative Commons Attribution-NonCommercial License](https://creativecommons.org/licenses/by-nc/4.0/), which permits use, distribution and reproduction in any medium, provided the original work is properly cited and is not used for commercial purposes.

Abstract Influenza epidemics, a major contributor to global morbidity and mortality, are influenced by climate factors including absolute humidity and temperature. Climate change is expected to increase the frequency and severity of climate extremes, potentially impacting the duration and magnitude of future influenza epidemics. However, the extent of these projected effects on influenza outbreaks remains understudied. Here, we use an epidemiologic model adapted for temperate and tropical climates to explore how climate variability may affect seasonal influenza. Using climate anomalies derived from historical data, we found that simulated periods of anomalous climate conditions impacted both the projected influenza outbreak peak size and the total proportion infected, with the strongest effects observed when the anomaly was included just before the typical peak. Effects varied by climate: temperate regions showed a unimodal relationship, while tropical climates exhibited a nonlinear pattern. Our results emphasize that the intensity of weather extremes is key to understanding how climate change may affect influenza outbreaks, laying the groundwork for utilizing weather variability as a potential early warning for influenza activity.

Plain Language Summary Influenza epidemics represent a persistent global public health issue and are impacted by climate drivers including absolute humidity and temperature. Climate variability is projected to increase under climate change, yet there is limited understanding how it may impact influenza transmission. We assess how climate variability may impact future influenza outbreaks in temperate and tropical climates with epidemiological models. Using influenza and climate data, we incorporate periods of anomalous climate conditions into the model. By comparing the anomalous peak size and total proportion infected to the expected baseline peak and total proportion infected, we calculate the relative difference in peak size and proportion infected attributed to the anomaly. When anomalous climate conditions occurred before the typical outbreak, a low anomaly was associated with a relative increase in peak size, whereas a high anomaly resulted in a smaller peak size. We also find the relationship between the anomaly and outbreak size varied by climate zone: outbreaks in temperate areas were most sensitive to climate anomalies prior to the influenza peak, whereas anomalies in tropical areas impacted outbreaks year-round. Our findings demonstrate the importance of considering climate variability as a distinct element of the broader impacts of climate change on future influenza outbreaks.

1. Introduction

Influenza infections account for considerable morbidity and mortality around the globe each year, resulting in an estimated 3–5 million cases of serious disease and 290,000–650,000 deaths (Mackenzie, 2024). The climate plays a crucial role in determining the timing and severity of these outbreaks, however the association differs by region (Lowen et al., 2007; Shaman & Kohn, 2009; Shaman et al., 2010; J. D. Tamerius et al., 2013). Climate change is expected to alter patterns in weather variability in the coming years (Bathiany et al., 2018; Field et al., 2012; Intergovernmental Panel On Climate Change, 2022; Johnson et al., 2018), which may have implications for the timing and magnitude of seasonal influenza outbreaks. There is limited understanding of how climate variability, particularly climate extremes, will affect influenza epidemics (Flahault et al., 2016; Gilbert et al., 2008; Mirsaiedi et al., 2016; Prosser et al., 2023). Understanding how weather extremes may impact seasonal influenza patterns is important for public health planning to mitigate influenza burden under the effects of climate change.

Temperate areas experience seasonal influenza epidemics during the winter months, while tropical regions have influenza activity throughout the year or experience seasonal peaks during the rainy season (Bloom-Feshbach

et al., 2013; Martinez, 2018; J. Tamerius et al., 2011; Viboud, Alonso, & Simonsen, 2006; Viboud, Bjørnstad, et al., 2006). In temperate regions, epidemiological and laboratory-based studies have found that the lower absolute humidity during wintertime induces conditions that promote the viability and transmission of the influenza virus (Paynter, 2015; Shaman & Kohn, 2009; Shaman et al., 2010; J. Tamerius et al., 2011; J. D. Tamerius et al., 2013). While there are additional climate factors (e.g., temperature (Lowen et al., 2008), solar radiation (Hessling et al., 2022)) and social factors (e.g., increased indoor contact (Cauchemez et al., 2008)) that help explain some variations in influenza seasonality, absolute humidity remains the strongest known predictive factor to account for seasonal influenza patterns in temperate areas. In tropical regions, the relationship between climate variables and influenza transmission remains less studied, although absolute humidity and temperature appear to be strongly influential. Work investigating influenza transmission in Hong Kong, a tropical environment, found evidence of a bimodal relationship between the effects of temperature and absolute humidity (Yuan et al., 2021), and these findings have since been validated in research focused on influenza transmission in Bangladesh (Mahmud et al., 2023). Understanding the distinct impact of climate extremes in both temperate and tropical regions is crucial for public health planning in these settings.

Here we use two epidemiological influenza models—a temperate model driven by absolute humidity, and a tropical model driven by absolute humidity and temperature—to explore how extreme weather patterns could impact influenza outbreaks in urban areas. We initially model impacts in two temperate locations (Manhattan, NY, and San Francisco, CA), and two tropical locations (Dhaka, Bangladesh and Hong Kong, special administrative region of China). Of the two temperate locations, Manhattan has a larger range of absolute humidity values through the year, while San Francisco experiences relative climate stability with a smaller range of absolute humidity. Both Manhattan and San Francisco generally experience influenza outbreak peaks that overlap with periods of low absolute humidity. In the two tropical locations, the large influenza outbreak in Dhaka historically overlaps with periods of high temperature and absolute humidity, whereas in Hong Kong, the primary outbreak occurs during periods of low temperature and absolute humidity, with additional smaller outbreaks at periods of high temperature and absolute humidity. Building on previous work, we assume that low absolute humidity increases transmission in temperate locations, and a non-linear combination of temperate and absolute humidity impact transmission in tropical locations. By incorporating periods of anomalously low or high absolute humidity (and temperature for the tropical locations) at different time points, in influenza models calibrated to each location, we explore the potential effect of climate extremes on the seasonal outbreak size and total proportion infected.

2. Materials and Methods

2.1. Influenza Data

Data on confirmed weekly influenza hospitalizations in the United States were derived from the State Inpatient Databases (SID), sponsored by the Agency for Healthcare Research and Quality (AHRQ) as part of the Healthcare Cost and Utilization Project (HCUP) (HCUP-US Home Page, 2024; Jacobs et al., 2014). The SID contains information relating to all community hospitals at a county-level resolution from 1988 to 2010, with data spanning 22 influenza seasons. Hospitalization data from 2009, the year of the H1N1 swine flu pandemic, was excluded to focus the analysis on seasonal patterns of influenza outbreaks. We took weekly influenza hospitalization time series from San Francisco and Manhattan for initial model fitting. To address potential year-to-year variations in vaccination coverage and data reporting, we calculated weekly mean influenza infections over the whole study period and normalize cases such that maximum is one. Data on confirmed influenza cases in Bangladesh were obtained from the Institute of Epidemiology, Disease Control and Research, Bangladesh, as reported in Mahmud et al. (2023). Monthly mean influenza burden was calculated for the Dhaka district in Bangladesh. Data on confirmed influenza cases from 2014 through 2019 were obtained from the Center for Health Protection of the Hong Kong Special Administrative Region.

2.2. Climate Data

Daily temperature and dew point temperature data from 1980 to 2015 were downloaded from the ERA5 gridded hourly data set on single levels with 0.25×0.25 resolution, representing approximately 30 km^2 grids. ERA5 data is a combination of observed satellite values and projected climate variables to create a comprehensive and standardized global data set. Daily average temperature and absolute humidity were computed for New York, San

Francisco, and Dhaka from the ERA5 data set. Climate data for Hong Kong were derived from the Hong Kong observatory, as reported in Yuan et al. (2021). The Clausius-Clapeyron relation enabled calculation of mean absolute humidity from temperature and dew point temperature, a measure of volume of water per volume of air. Due to the relatively shorter time series of Hong Kong, the climate data were smoothed. For all locations, weekly values and the mean weekly value for climate variables were calculated to obtain the anomaly. Weekly climate anomalies were calculated by subtracting the week mean from each weekly value, resulting in a data set where positive values indicate a higher-than-average weekly absolute humidity, and negative values indicate a lower-than-average weekly absolute humidity. For the tropical locations, daily mean climate values were also calculated to be used in the model. Mean absolute humidity for the main temperate locations are visualized in Figure S6 in Supporting Information S1 and mean absolute humidity and temperature for the tropical locations are shown in Figure S7 in Supporting Information S1.

2.3. Mechanistic Model With Climate

As the dynamics of infectious disease rely on individuals moving between the susceptible, infected, and recovered categories, mechanistic models are used to capture the non-linear relationships. We used two models to explore the possible impact of climate extremes on influenza outbreaks. The first model was developed for temperate climates and is dependent on absolute humidity, and the second model was developed for tropical climates and is dependent on absolute humidity and temperature. Both models rely on the canonical Susceptible-Infected-Recovered framework with transmission governed by the following equations:

$$\frac{dS}{dt} = \frac{N - S - I}{L} - \beta(t) \frac{S * I}{N} \quad (1)$$

$$\frac{dI}{dt} = \beta(t) \frac{S * I}{N} - \frac{I}{D} \quad (2)$$

Where N is the total population size, S is the susceptible population, I is the infected population, and D is the mean infectious period. L is the duration of immunity and is set to 40 weeks, enabling the influenza epidemic to recur seasonally. $\beta(t)$ represents the contact rate at time t , and is related to the basic reproductive number (R_0) in this framework by $R_0(t) = \beta(t) D$. For the temperate model developed by Shaman et al. (2010) for locations across the United States, $R_0(t)$ is dependent on absolute humidity $q(t)$ as:

$$R_0(t) = \exp(-180 * q(t) + \log(R_{0\max} - R_{0\min})) + R_{0\min} \quad (3)$$

Where $R_{0\max}$ and $R_{0\min}$ are the maximum and minimum effective reproductive number. The SIR framework described here for temperate climates models output data on a weekly cadence. Parameters were identified by calibrating the model to observational influenza surveillance data. For the tropical model, developed by Yuan et al. (2021) for Hong Kong, $R_0(t)$ is dependent both on absolute humidity $q(t)$ and temperature $T(t)$ as:

$$R_0(t) = [aq(t)^2 + b(q)^2 + c] \left(\frac{T_c}{T(t)} \right)^{T_{\exp}} \quad (4)$$

Where a, b, c are defined in Equations 5–7, q_{\max} is the absolute humidity (g/kg) value at which $R_0 = R_{0\max}$ when $T = T_c$ and represents the maximum absolute humidity allowed, q_{\min} is the absolute humidity (g/kg) value at which $R_0 = R_{0\max}$ when $T = T_c$ and represents the minimum absolute humidity allowed, q_{mid} is the absolute humidity at which $R = R_{0\max} - R_{0\text{diff}}$, $R_{0\text{diff}}$ is the difference between $R_{0\max}$ and R_0 when $q = q_{\text{mid}}$, T_c is the critical temperature below which changes in temperature do not impact transmission, and T_{\exp} determines the strength of the relationship between temperature and R_0 .

$$a = \frac{-b}{q_{\max} + q_{\min}} \quad (5)$$

$$b = \frac{(R_{0\max} - (R_{0\max} - R_{0\text{diff}}))(q_{\max} + q_{\min})}{(q_{\max} - q_{\text{mid}})(q_{\min} - q_{\text{mid}})} \quad (6)$$

$$c = (R_{0\max} - R_{0\text{diff}}) - aq_{\text{mid}}^2 - bq_{\text{mid}} \quad (7)$$

The SIR framework described here for tropical climates models output data on a daily cadence.

2.4. Model Optimization

Parameters representing fundamental features of the influenza pathogen (D , L) were held constant at values based on prior work by Shaman et al. (2010), while parameters related to the reproduction number, which is expected to vary by location due to differences in contacts, were estimated to capture average effects across the study period. Best fit model parameters were estimated for the temperate model using a grid search of a range of values based on the literature for $R_{0\min}$ and $R_{0\max}$ by fitting the model to observed influenza hospitalization data (Table S1, Figure S4 in Supporting Information S1). Best fit was assessed by minimizing the mean average error between the observed and simulated weekly infection values for each county (Table S2, Figure S5 in Supporting Information S1). Each simulation was run with a burn-in period to account for transient dynamics.

Best fit model parameters were estimated for the tropical model by testing a range of parameter values and tuning the model to the observed influenza infection data. Parameters that were fit include: $R_{0\max}$, $R_{0\text{diff}}$, q_{\min} , q_{\max} , q_{mid} , T_C , T_{exp} , D , L , S_0 , and I_0 . There were 5,000 parameter combinations generated by latin hypercube sampling (LHS) based on parameter ranges from the literature (Table S3 in Supporting Information S1). There were 5,000 simulations run for Dhaka and Hong Kong based on the parameter combinations, and best fit was assessed by minimizing the error between the observed and simulated infection values. From the initial 5,000 parameter combinations, we used an iterative process to select the best fit parameters. For each location, we picked the top 500 parameter combinations with the lowest root mean square error (RMSE), and then created a 95% high density interval (HDI) for each parameter. We then used the new 95% HDI to create a new range of parameter values if the upper (or lower) bound was outside 10% of the original parameter maximum (or minimum) value. From here, we recreated 5,000 parameter combinations with LHS with the newly identified parameter range and repeated the simulations for each location. The tuning was completed when the parameter ranges did not decrease and were within 10% of the 95% HDI bounds. Dhaka underwent 10 rounds of model tuning, and Hong Kong underwent 13 rounds of model tuning. We report the best-fit parameters (Table S3 in Supporting Information S1) and provide the top ten best-fit parameter combinations (Figure S6 in Supporting Information S1) for each location. Each simulation was run with a burnin period to account for transient dynamics.

2.5. Anomaly Inclusion Into Model

To examine the impact of weather extremes on modeled influenza outbreaks, we incorporated periods of anomalous climate conditions into the model. An anomaly is defined as the percentile departure from the average climate conditions (Global Surface Temperature Anomalies | National Centers for Environmental Information (NCEI), 2024). To identify anomaly values, we first calculated the average weekly temperature and specific humidity for each study location over the study period. Anomalies were then computed as the difference between the value for each individual week across all years in the study period and the corresponding average weekly value. This process generated an anomaly range for each location and climate variable. For instance, a 1-week 1% climate anomaly during epidemiologic week 10 is calculated by adding a 1st percentile anomaly value to week 10 (as anomalies are deviations from the climatology, we add this directly the weekly average). We replaced every week in the year with anomalous conditions, with the anomaly percentiles ranging from the 1st through the 99th specific to each location. We also extended the anomaly duration by introducing periods of two, three, and four consecutive weeks of anomalous conditions into the model for the 1st and 99th percentile anomalies.

For temperate regions in this analysis, which experience one outbreak per year, peak size serves as an effective measure of anomaly impact. For tropical locations with extended influenza transmission, the total proportion infected, represented as area under the curve (AUC), better reflects the impact of a climate anomaly. To isolate any anomaly effects, we defined the analysis year as starting the day the anomaly is included and ending 52 weeks later. This rolling timeframe enabled analysis of late-year anomalies and their effect on outbreaks in the following year. From the model outputs, we identified the maximum projected peak in the anomaly model and compared it to the baseline peak. We standardized this difference by dividing the anomaly peak by the baseline peak, resulting in the relative peak size difference. Similarly, we calculated the AUC for both anomaly and baseline conditions and standardized the anomaly AUC against the baseline.

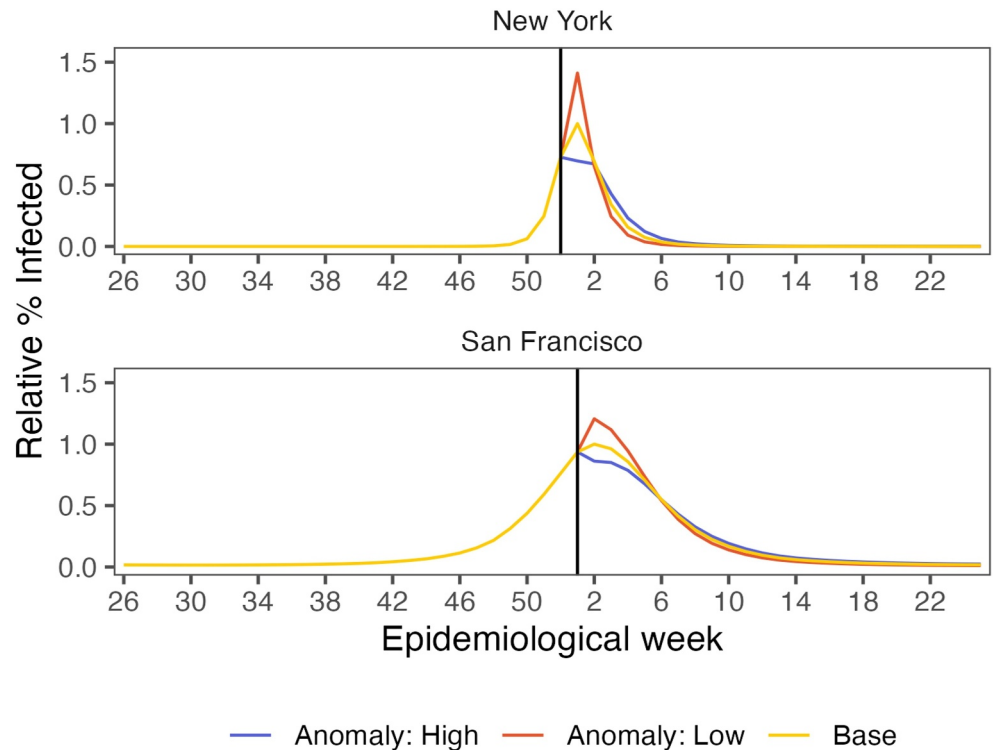


Figure 1. Predicted impact of climate extremes on the seasonal influenza outbreak in Manhattan, NY and San Francisco, CA. Impact of 1 week of 1% (red line) and 99% (blue line) anomalous absolute humidity in Manhattan and San Francisco. The anomaly was added during the week that would have the maximum impact on the outbreak. The black vertical line indicates the week of anomalous absolute humidity, and the yellow line indicates the expected baseline outbreak.

Data processing and analysis was performed using R version 4.3.1 and RStudio version 2023.06.1 + 524.

3. Results

3.1. Temperate Model

In Figure 1 we show the timeline for the effect of the anomaly in the week that had the greatest impact on influenza outbreak size relative to baseline projections in Manhattan, New York and San Francisco, California. In each location, the presence of an anomalously low week of absolute humidity just prior to the peak of the influenza outbreak was associated with an increase in the infected peak size (red line) relative to baseline projections (yellow line). In contrast, the presence of an anomalously high week of absolute humidity at the same time was associated with a decrease in the infected peak size (blue line) relative to baseline projections (yellow line). The x-axes in Figure 1 are shifted to center the main influenza outbreak for the temperate locations.

We find that a single week of a 1% absolute humidity anomaly just prior to the influenza outbreak leads to a predicted 41.1% increase in relative peak size in Manhattan and an 18.7% increase in relative peak size in San Francisco. Inclusion of a single week of anomalously low absolute humidity conditions had a larger effect on the relative peak size when compared to a week of anomalously high absolute humidity. A single week of 99% absolute humidity prior to the influenza outbreak led to predicted smaller outbreaks in Manhattan and San Francisco, corresponding to 27.4% and 12.8% relative decreases in peak size.

Figure 2a portrays how a single anomalous week of absolute humidity could impact the projected influenza peak in the year following the anomaly in Manhattan, and Figure 2c depicts the same analysis for San Francisco. The x-axes in Figure 2 are shifted to center the main influenza outbreak for the temperate locations, similar to Figure 1. Blue shading indicates that the inclusion of an anomaly resulted in a predicted smaller outbreak size relative to baseline, and red shading indicates the inclusion of the anomaly resulted in a predicted larger outbreak size relative to baseline. Both temperate locations assessed exhibited similar patterns in the effect of timing and

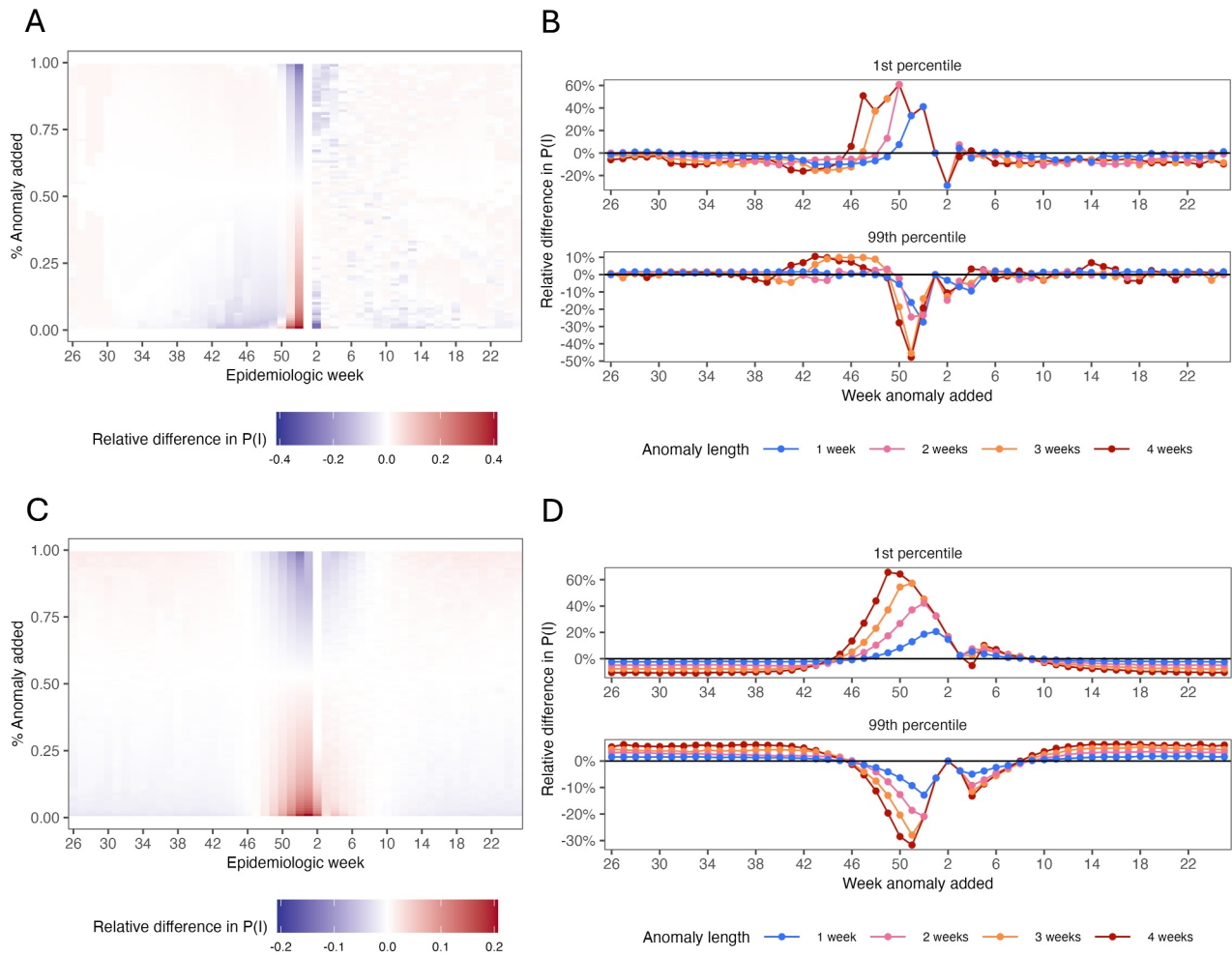


Figure 2. Surface and wave plots for Manhattan, NY and San Francisco, CA. (a) Projected relative peak size difference for Manhattan for 1%–99% anomalies added during each epidemiologic week. (b) Relative peak size increases for Manhattan for 1% and 99% anomalies over 1–4 consecutive week durations. (c) Projected relative peak size difference for San Francisco for 1%–99% anomalies added during each epidemiologic week. (d) Relative peak size increases for San Francisco for 1% and 99% anomalies over 1–4 consecutive week durations.

direction of the anomaly. The inclusion of a week of anomalously low absolute humidity just prior to the projected peak of the outbreak resulted in the largest increase in the relative peak size compared to baseline, likely due to the onset of favorable conditions spurring influenza transmission. However, if a week of anomalously high absolute humidity occurred at that same time, the projected outbreak size was smaller compared to the baseline expectation, likely due to higher absolute humidity dampening influenza transmission. The inclusion of an anomalously low week of absolute humidity in the weeks leading to the outbreak resulted in a seasonal outbreak peak smaller than expected under baseline conditions, likely due to increased transmission at the anomaly time reducing the susceptible pool at the typical outbreak peak. In contrast, a period of anomalously high absolute humidity during this same time period led to a larger seasonal outbreak peak than expected under baseline conditions. We believe this may be due to the high absolute humidity resulting in decreased influenza activity at the time of the anomaly, resulting in a larger pool of the susceptible population during the outbreak peak. Effect sizes resulting from the inclusion of the climate anomaly were more pronounced in New York than San Francisco, which may be driven by greater variation of anomaly values as observed in the historic climate data (Figure S1 in Supporting Information S1). In addition, we found that greater severity of the minimum climate anomaly was associated with a larger difference in relative peak size in 36 locations assessed across the United States (Figure 7).

We also investigated how the inclusion of multiple weeks of anomalous climate conditions were projected to impact the influenza outbreak. Figure 2b portrays how anomalous periods of one through four consecutive weeks

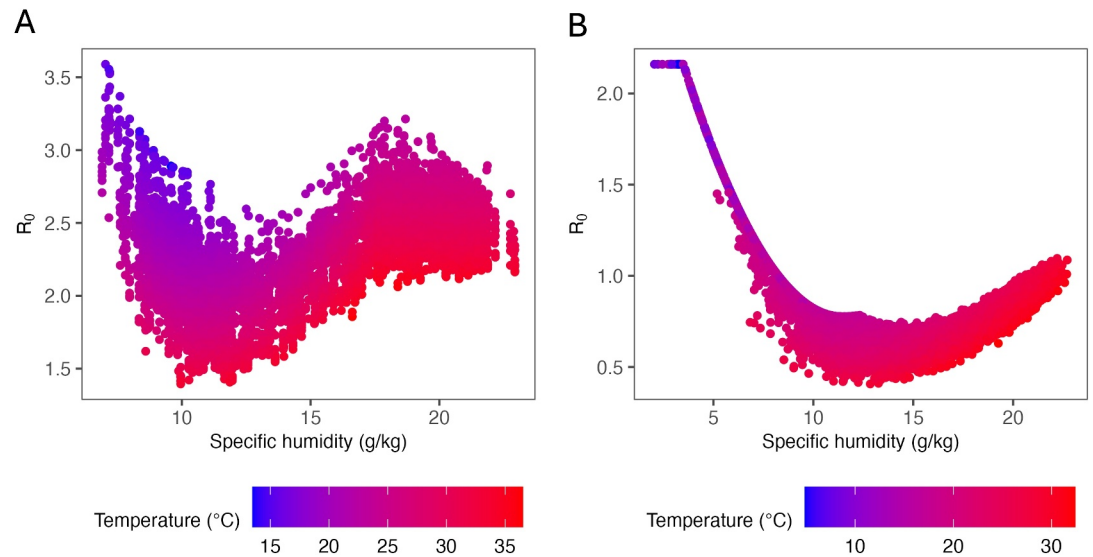


Figure 3. Basic reproductive number (R_0) values for Dhaka and Hong Kong. (a) R_0 predicted from temperature and absolute humidity values for Dhaka, 1985–2014. (b) R_0 predicted from temperature and absolute humidity values for Hong Kong, 1998–2019.

of anomalously high or low absolute humidity were projected to impact the relative difference in peak size between the anomalous and baseline models for Manhattan, and Figure 2d portrays the same calculations for San Francisco. Generally, longer periods of anomalous climate conditions exacerbated the effects observed under shorter periods of anomalous climate conditions. For each location, we found that the most substantial impacts on the predicted peak size overlapped with the weeks leading to the outbreak peak. A 1% anomaly added just after the outbreak peak was projected to decrease the maximum anomaly peak over the next year, likely due to extended influenza transmission decreasing the susceptible pool for the upcoming influenza season. Visualized effects of the anomaly inclusion were smoother in San Francisco than in Manhattan, as seen in the wave shape in Figure 2d compared to the more pronounced bumps in Figure 2b.

3.2. Basic Reproductive Number Calculation in Tropical Locations

As in Yuan et al. (2021), we fitted the relationship between influenza transmission and climate factors (absolute humidity, temperature) by calculating the basic reproductive number (R_0) for Dhaka (Figure 3a) and Hong Kong (Figure 3b) using the best-fit parameters for each location. Figure 3 shows a non-linear relationship between absolute humidity and R_0 , with higher predicted transmission in both cold, low-absolute humidity and hot, high-absolute humidity. Introducing anomalous climate conditions during these outbreaks affected the calculated contemporaneous R_0 values. Depending on the climate conditions when an anomaly was included, the figures demonstrate how a 1% anomaly may boost transmission if occurring during a cold, low-absolute humidity period and may dampen transmission if occurring during a hot, high-absolute humidity period. These results highlight that tropical locations with wide annual ranges of temperature and absolute humidity may have two periods of higher transmission, potentially vulnerable to climate extremes: cold, low-absolute humidity and hot, high-absolute humidity.

3.3. Tropical Model

We find large unimodal effects of a single anomalous week of absolute humidity in temperate model analyses; however, distinct climate drivers are expected to be influential in tropical locations. Using a model previously developed for Bangladesh, we explored the impact of climate variability on influenza epidemics in Dhaka and Hong Kong. Figure 4 shows the timeline of the impact of the anomaly during the week with the greatest effect on outbreak peak size for Dhaka (4a) and Hong Kong (4b). In Dhaka, a single week of 1% anomalously low absolute humidity and temperature before the influenza outbreak increased the infected peak size (red line) by 24.8% relative to baseline projections (yellow line). Conversely, a single week of anomalously high temperature and

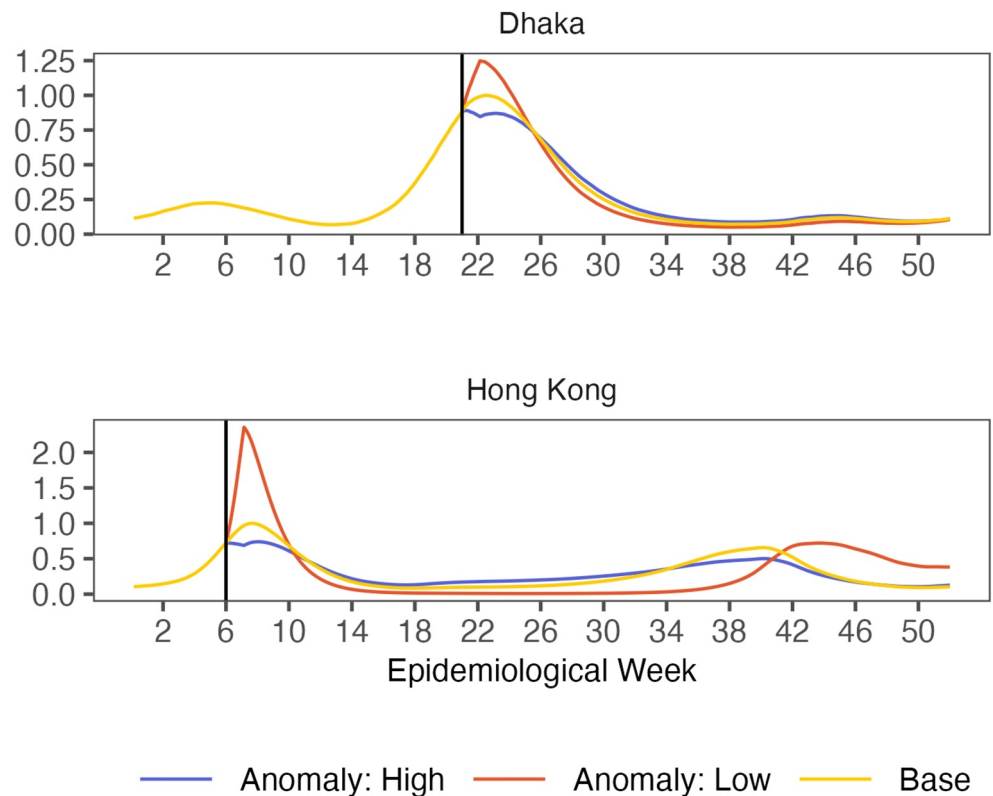


Figure 4. Predicted impact of climate extremes on the seasonal influenza outbreak in Dhaka, Bangladesh and Hong Kong. The anomaly was added during the week that would have the maximum impact on the outbreak. The black line indicates the beginning of the week of anomalous absolute humidity and temperature. (a) Impact of 1 week of 1% anomalous absolute humidity and temperature in Dhaka, Bangladesh. (b) Impact of 1 week of 1% anomalous absolute humidity and temperature in Hong Kong.

absolute humidity at the same time period reduced the infected peak size (blue line) by 22.8%. For Hong Kong, a single week of 1% anomalously low temperature and absolute humidity increased the predicted relative peak size by 135.6%, while a week of a 99% anomalous temperature and absolute humidity led to a 25.2% decrease in predicted relative peak size. Both locations showed similar effects to the analysis in temperate locations when the anomaly occurred around the historic outbreak peak: low temperature and absolute humidity anomalies led to larger outbreaks, whereas high anomalies dampened them. In the tropical locations, including a week of 99% anomalously high temperature and absolute humidity produced a bimodal outbreak pattern, with a moderate initial peak followed by a smaller one. This bimodal effect was observed in both Dhaka and Hong Kong, and is seen in the blue line in Figure 4.

When examining the impact of climate extremes on projected influenza outbreaks in tropical climates, we considered the hypothesized non-linear relationship between climate variables and transmission. Figure 3 showed the increased influenza transmission both at cold, low-absolute humidity and at hot, high-absolute humidity. To study this non-linear effect, we used the same methods as described for the temperate model to analyze the impact of 1st–99th percentile temperature and absolute humidity anomalies on the relative outbreak size. Figure 5a illustrates how the timing of a single week of anomalous climate conditions affects the projected peak in Dhaka, while Figure 5c depicts the same analysis for Hong Kong. A 1% temperature and absolute humidity anomaly during the outbreak peak increased the basic reproductive number (R_0), leading to a larger peak relative to baseline conditions in both locations. In Dhaka, adding a 1% temperature and absolute humidity anomaly of two or more weeks during periods of cold, low-absolute humidity resulted in a larger projected peak, highlighting the strong influence of these conditions on influenza transmission. In Hong Kong, a 1% temperature and absolute humidity anomaly had large effects, particularly when they overlapped with cold and low-absolute humidity climate conditions. This finding is likely due both to low temperature and absolute humidity boosting

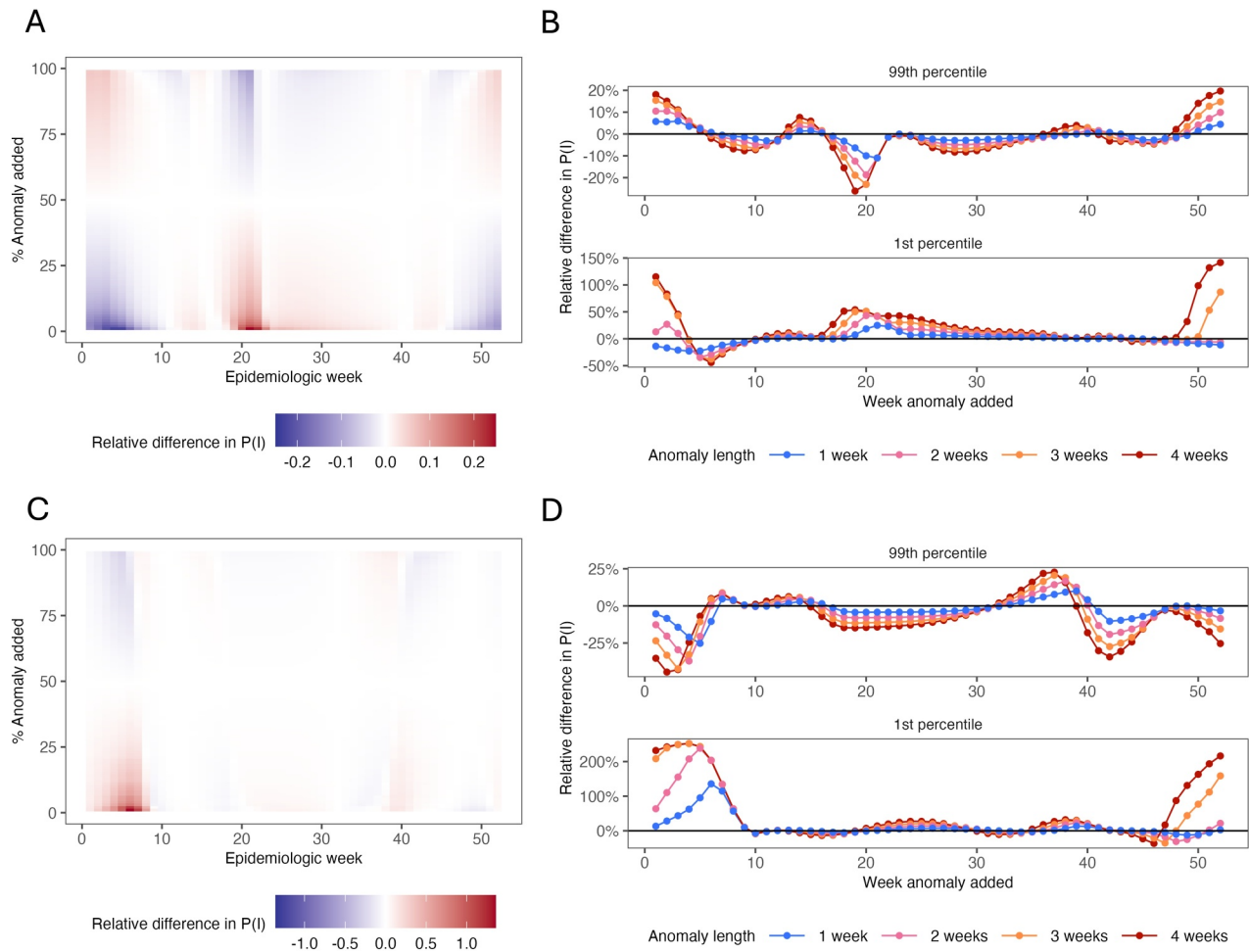


Figure 5. Surface and wave plots relating to peak size for Dhaka, Bangladesh and Hong Kong, special administrative region of China. (a) Projected relative peak size difference for Dhaka for 1%–99% anomalies added during each epidemiologic week. (b) Relative peak size increase for Dhaka for 1% and 99% anomalies over 1–4 consecutive week durations. (c) Projected relative peak size difference for Hong Kong for 1%–99% anomalies added during each epidemiologic week. (d) Relative peak size increase for Hong Kong for 1% and 99% anomalies over 1–4 consecutive week durations.

transmission and the presence of a larger susceptible population relative to other times in the year. A 99% temperature and absolute humidity anomaly during the outbreak peak decreased R_0 , leading to a smaller peak relative to baseline conditions in both Dhaka and Hong Kong.

We also examined how multiple weeks of anomalous climate extremes affected the influenza outbreak, similar to our analysis of the temperate model. Figure 5b illustrates the projected relative differences in peak size for Dhaka with the addition of one to four consecutive weeks of 1% or 99% temperature and absolute humidity anomalies, and Figure 5d shows the same for Hong Kong. In both locations, longer durations of anomalous conditions intensified the effects observed with shorter durations. The strong bimodal relationship observed in Figure 5a is further demonstrated in Figure 5b, where the 1% temperature and absolute humidity anomaly shows an increasing effect size with longer anomaly periods in Dhaka. The 99% temperature and absolute humidity anomaly had a nonlinear impact, where two periods led to a reduced peak size compared to the baseline. Interestingly, both 1% and 99% temperature and absolute humidity anomalies lasting at least 2 weeks early in the year increased the outbreak peak in Dhaka, albeit through different mechanisms. The 1% temperature and absolute humidity anomaly spurred early transmission, leading to a larger early peak, while the 99% anomaly lowered transmission and created a larger susceptible pool for a peak later in the year. In Hong Kong, the 1% temperature and absolute humidity anomaly had significant effects on the projected peak size, which grew as its duration extended. Inclusion of 1 week of a 99% temperature and absolute humidity anomaly resulted in a smaller peak when aligned with the primary outbreak period.

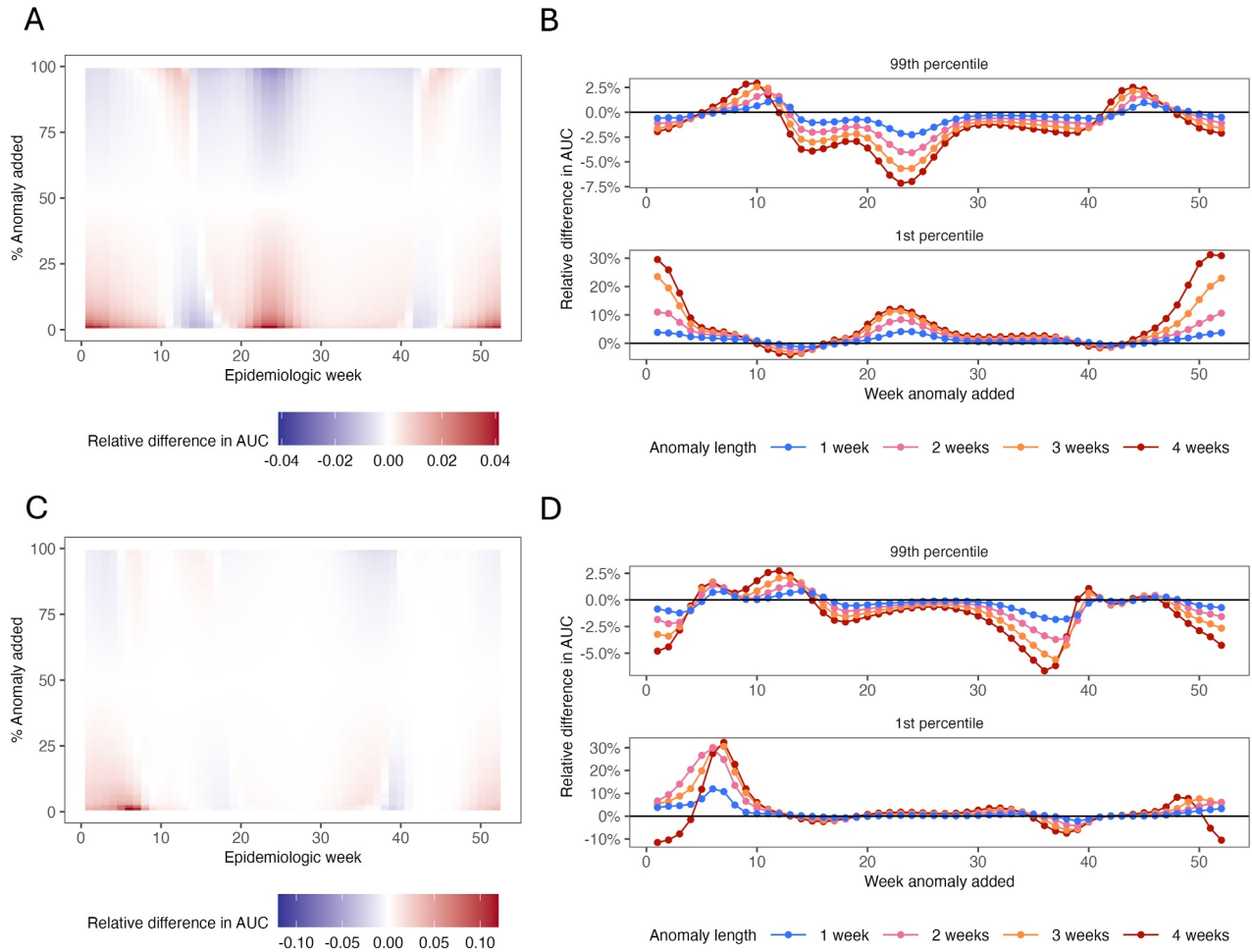


Figure 6. Surface and wave plots relating to area under the curve (AUC) for Dhaka, Bangladesh and Hong Kong, special administrative region of China. (a) Projected AUC difference for Dhaka for 1%–99% anomalies added during each epidemiologic week. (b) Relative AUC increase for Dhaka for 1% and 99% anomalies over 1–4 consecutive week durations. (c) Projected relative AUC difference for Hong Kong for 1%–99% anomalies added during each epidemiologic week. (d) Relative AUC increase for Hong Kong for 1% and 99% anomalies over 1–4 consecutive week durations.

To compare the total proportion infected between climate conditions, we calculated the area under the infected curve. Figure 6 uses the same anomaly projections as in Figure 5 to compare the total proportion infected in the anomaly model compared to the baseline model for each anomaly week combination. Figure 6a shows the impact of adding a temperature and absolute humidity anomaly during any given week on the total proportion infected for the year in Dhaka, while Figure 6c depicts the same for Hong Kong. In Dhaka, 1 week of anomalously low temperature and absolute humidity had varied impacts, with three distinct periods increasing the proportion infected and three periods decreasing it. The largest increase (4.1%) occurred when a 1% temperature and absolute humidity anomaly was added in week 3, a time of historically colder temperature and lower absolute humidity in Dhaka. In Hong Kong, a 1-week 1% temperature and absolute humidity anomaly had the most significant impact when included around the major outbreak, with smaller effects at other times. The largest increase (11.9%) occurred when a 1% temperature and absolute humidity anomaly was added in week 4, a period of colder temperature and lower absolute humidity in Hong Kong.

We also examined the impact of varying lengths of anomalous temperature and absolute humidity on the total proportion infected with influenza in the tropical locations. Figure 6b shows the effects of one through four consecutive weeks of 1% and 99% temperature and absolute humidity anomalies on the projected total proportion infected in Dhaka, and Figure 6d shows the same for Hong Kong. In both locations, longer periods of temperature and absolute humidity anomalies generally amplified the effects observed at shorter periods. The largest impacts

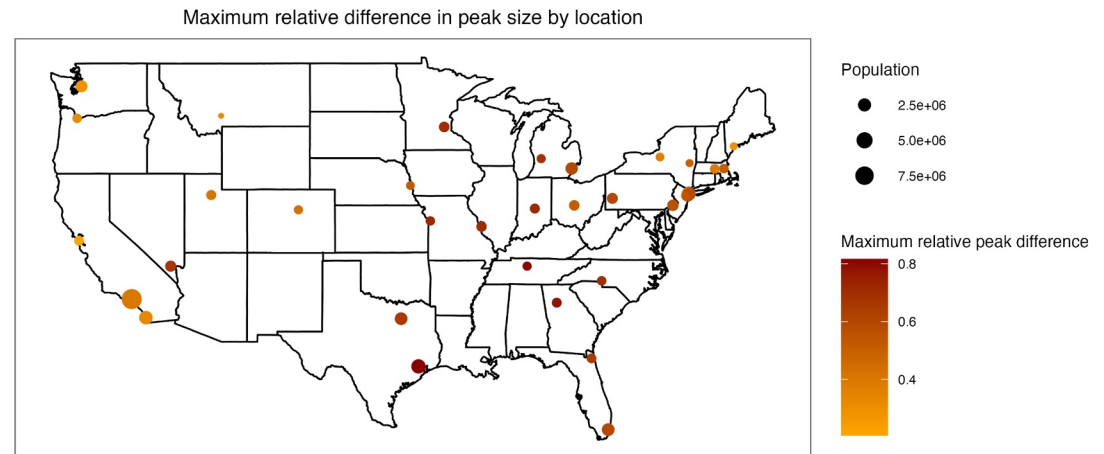


Figure 7. Spatial patterns of projected maximum difference in peak size by location in the United States. Projected differences in relative peak size resulting from the inclusion of a 1% absolute humidity anomaly at the maximum impact week for all locations analyzed in the United States.

were seen when typical climate conditions involved low temperature and absolute humidity, aligning with previous findings that these conditions are associated with higher influenza activity.

4. Discussion

To better understand how climate extremes in both temperate and tropical areas may impact the magnitude of the seasonal influenza outbreak, anomalous periods of one through four consecutive weeks of absolute humidity (and temperature for the tropical locations) were incorporated into the model, and the differences in peak size and total proportion infected relative to baseline projections were calculated. In each location, there was one highly influential week that corresponded to the greatest relative difference in peak size following the inclusion of a 1% or a 99% anomaly of absolute humidity (and temperature for tropical climates). In temperate locations, 1 week of 1% anomalous absolute humidity at this time was associated with a predicted relative increase in influenza peak size, whereas a week of a 99% anomalous absolute humidity reduced the influenza peak size. In tropical locations, the impact of anomalous temperature and absolute humidity was largely dependent on the current climate, as favorable conditions for influenza transmission occurred at both high and low combinations of temperature and absolute humidity. Interestingly, a larger outbreak peak size did not always correspond to a larger total proportion infected: in Dhaka, the maximum impact of a 1-week 1% temperature and absolute humidity anomaly resulted in a 24.8% larger predicted peak size compared to baseline, but the total proportion infected was 1.6% less than the total predicted proportion infected under baseline conditions. Increasing the length of the anomalous climate period generally exacerbated the pattern that was identified under 1 week of anomalous climate conditions. Climate anomalies incorporated into the model in the months prior to the highly influential week had an opposite sign effect on the projected difference in peak size. We believe many of these shifts were driven by changes to the susceptible pool resulting from the inclusion of the anomaly. In Dhaka, if a 1% absolute humidity and temperature anomaly spurred transmission early in the year outside the main outbreak, this would lead to a smaller susceptible pool later on during the main outbreak. In contrast, a 99% absolute humidity and temperature anomaly at that same time could dampen transmission, resulting in a larger susceptible pool during the main outbreak. These patterns were consistently identified across the 36 additional locations analyzed (Figure S2 in Supporting Information S1).

Other analyses have evaluated the relationship between seasonal influenza outbreaks and the climate variables in tropical locations. Unlike seasonal influenza outbreaks in temperate regions, which are characterized by a peak of infection during the dry and winter months, tropical areas experience persistent influenza outbreaks throughout the year. There is a hypothesized nonlinear relationship between absolute humidity and the reproductive number in tropical regions, modified by temperature at higher levels of absolute humidity (Yuan et al., 2021). In the results, we see evidence for this nonlinear relationship in the multiple periods of the year in which a 99% or 1% temperature and absolute humidity anomaly results in an increased peak size (Figure 5). This pattern is not present in the temperate location analysis, for which the only periods of the year we found to be very susceptible to a high

or low absolute humidity anomaly were immediately surrounding the major outbreak. Considering current climate change projections, it is possible that more areas, including in historically temperate regions, will move toward tropical climates in the United States (Osland et al., 2021). Under this regime, it is likely that patterns of seasonal influenza outbreaks will also shift, and tropical locations may be increasingly susceptible to periods of climate variability (Field et al., 2012). For these reasons, understanding the mechanisms behind influenza activity we currently witness using the tropical model are important for validating the results.

4.1. Limitations and Strengths

There are several caveats with this analysis. First, the model is implicitly fit to a semi-vaccinated population, but a vaccination parameter is not explicitly incorporated into the model. If a universal vaccine became available, this could impact patterns of transmission not currently accounted for in the model. Second, this work does not account for different influenza strains, for which changing circulation patterns could alter the magnitude of the influenza outbreak. Third, this analysis is focused on outcomes in four locations (Manhattan, NY, San Francisco, CA, Dhaka, Bangladesh, and Hong Kong, special administrative region of China). However, an additional 36 locations across the United States were analyzed (Table S2 in Supporting Information S1), and the broad patterns identified with Manhattan and San Francisco were consistent between the additional locations (Figures S2 and S3 in Supporting Information S1). Broad patterns in maximum relative peak size associated with inclusion of an anomaly are seen in Figure 7. Fourth, while the models were calibrated to each location based on historic climate and influenza data, additional work is required to characterize the relationship as causal. Our analysis investigates predicted outbreak patterns under variable climate conditions based on an epidemiological model, the results do not represent statistical estimates of an observed response to extremes.

5. Conclusions

There are mounting concerns regarding how climate change will impact future influenza outbreaks. Our analysis provides a step toward understanding how climate variability stands to affect the seasonal influenza outbreak across temperate and tropical climates. We found that elements such as severity of an anomalous climate period stand to be highly influential on the seasonal influenza outbreak, and that the direction and magnitude of the effects depended on the timing and climate of the outbreak. We also found locations that historically experienced greater climate variability had larger magnitude effect sizes on the simulated influenza outbreak when weather anomalies were included. The modeled effects of climate variability on the seasonal influenza outbreak also differed by climate. In temperate regions, we observed a unimodal relationship between the severity of an anomaly and its impact on the projected outbreak, whereas in tropical regions, influenza transmission was high under both cold, low-absolute humidity and hot, high-absolute humidity conditions. This suggests that while both temperate and tropical regions are vulnerable to climate variability, tropical locations in this analysis experienced multiple periods of heightened sensitivity while temperate locations experienced only one. This finding was further illustrated by comparing the total proportion infected: although a climate anomaly may not alter the maximum peak size, it can still affect the total infected population, with implications for healthcare system capacity and influenza-related mortality. While our study focused on dense urban areas, it is unlikely that the observed effects of the anomaly on outbreak peak are limited to a particular population density setting. There may be variation in the population size and mobility in less population dense locations, however this may be mitigated by calibrating the model to historic influenza and climate information. This analysis may be adapted in additional locations, and other model parameters may be included to account for differences in population density or mobility patterns.

Accounting for climate change impacts on infectious disease is vital for public health planning. In addition to preparing for shifts in outbreak patterns due to projected average weather changes, it is critical to also recognize the impact of climate variability on infectious disease outbreaks. While projections estimating average climate values help predict overall shifts in seasonal infectious disease patterns, climate variability is also expected to increase under climate change regimes (Field et al., 2012). Capturing the potential acute effects of climate anomalies on influenza outbreaks can inform public health preparation today and into the future as we continue to experience a changing climate. Our analysis found that a single week of anomalous absolute humidity just before the typical outbreak peak had a significant impact compared to other timings. Awareness of such anomalies could serve as a location-specific early warning for areas during influenza season (National Research Council (US) Committee on Climate, 2001). If a location experiences an anomalously low period of absolute humidity before

the typical influenza outbreak peak, public health officials can alert healthcare facilities about a potential increase in influenza transmission and cases. Extreme anomalies had a greater impact on relative outbreak size, highlighting the importance of preparing for increasing climate variability. More broadly, understanding the impact of extremes on infectious disease outbreaks is crucial as part of preparing for climate change.

Conflict of Interest

The authors declare no conflicts of interest relevant to this study.

Data Availability Statement

Influenza data were derived from 1988 to 2010 SID reporting, part of HCUP and sponsored by AHRQ. Climate data were extracted from the ERA5 gridded hourly data set on single levels. Data was downloaded and analyzed using open-source software. Python was used to extract climate data from the ERA5 gridded hourly data set (Python Software Foundation, 2024; C3S, 2018; Ecmwf/Cdsapi, 2019/2024). R was used for the statistical computing environment (version 4.3.1) to process, analyze, and visualize data (R Core Team, 2024). To extract the geographic data, we used raster and ncdf4 (Hijmans, 2023; Pierce, 2023). For data processing and visualization, we used tidyverse, reshape2, deSolve, lhs, lemon, and ggthemes (Arnold, 2024; Carnell, 2022; Edwards, 2024; Karlina Soetaert et al., 2010; Wickham, 2007; Wickham et al., 2019). Code and data to reproduce the main results are available at <https://github.com/aleksandrastamper/modeling-effects-clim-extremes>. Raw ERA5 data can be downloaded from <https://cds.climate.copernicus.eu/datasets/reanalysis-era5-single-levels?tab=overview> and AHQR data is available at <https://hcup-us.ahrq.gov/sidoverview.jsp> after signing a data use agreement.

Acknowledgments

The authors would like to acknowledge the Editor and anonymous reviewers for the manuscript.

References

- Arnold, J. B. (2024). ggthemes: Extra themes, scales and geoms for “ggplot2”. <https://CRAN.R-project.org/package=ggthemes>
- Bathiany, S., Dakos, V., Scheffer, M., & Lenton, T. M. (2018). Climate models predict increasing temperature variability in poor countries. *Science Advances*, 4(5), eaar5809. <https://doi.org/10.1126/sciadv.aar5809>
- Bloom-Feshbach, K., Alonso, W. J., Charu, V., Tamerius, J., Simonsen, L., Miller, M. A., & Viboud, C. (2013). Latitudinal variations in seasonal activity of influenza and respiratory syncytial virus (RSV): A global comparative review. *PLoS One*, 8(2), e54445. <https://doi.org/10.1371/journal.pone.0054445>
- C3S. (2018). ERA5 hourly data on single levels from 1940 to present [Dataset]. *Copernicus Climate Change Service (C3S) Climate Data Store (CDS)*. <https://doi.org/10.24381/CDS.ADBB2D47>
- Carnell, R. (2022). lhs: Latin hypercube samples. <https://CRAN.R-project.org/package=lhs>
- Cauchemez, S., Valleron, A.-J., Boëlle, P.-Y., Flahault, A., & Ferguson, N. M. (2008). Estimating the impact of school closure on influenza transmission from Sentinel data. *Nature*, 452(7188), 750–754. <https://doi.org/10.1038/nature06732>
- Ecmwf/cdsapi. (2024). [Python]. European Centre for Medium-Range Weather Forecasts. Retrieved from <https://github.com/ecmwf/cdsapi>
- Edwards, S. M. (2024). lemon: Freshing up your “ggplot2” Plots. <https://CRAN.R-project.org/package=lemon>
- Field, C. B., Barros, V., Stocker, T. F., & Dahe, Q. (2012). In *Managing the Risks of Extreme Events and Disasters to Advance Climate Change Adaptation: Special Report of the Intergovernmental Panel on Climate Change*. Cambridge University Press. <https://doi.org/10.1017/CBO9781139177245>
- Flahault, A., de Castaneda, R. R., & Bolon, I. (2016). Climate change and infectious diseases. *Public Health Reviews*, 37(1), 21. <https://doi.org/10.1186/s40985-016-0035-2>
- Gilbert, M., Slingenbergh, J., & Xiao, X. (2008). Climate change and avian influenza. *Revue Scientifique Et Technique (International Office of Epizootics)*, 27(2), 459–466.
- Global Surface Temperature Anomalies | National Centers for Environmental Information (NCEI). (2024). Retrieved from <https://www.ncei.noaa.gov/access/monitoring/global-temperature-anomalies>
- HCUP-US Home Page. (2024). Retrieved from https://hcup-us.ahrq.gov/?_gl=1*187oogj*_ga*MTgyMTMwMDQ1LjE3MzAzMDY1Njc*_ga_INPT56LE7J*MTczMDMwNjU2Ny4xLjAuMTczMDMwNjU2Ny4wLjAuMA
- Hessling, M., Gierke, A.-M., Sicks, B., Fehler, N., & Vatter, P. (2022). Sensitivity of influenza virus to ultraviolet irradiation. *GMS Hygiene and Infection Control*, 17, Doc20. <https://doi.org/10.3205/dgkh000423>
- Hijmans, R. J. (2023). raster: Geographic data analysis and modeling. Retrieved from <https://CRAN.R-project.org/package=raster>
- Intergovernmental Panel On Climate Change. (2022). *Climate change and land: IPCC special report on climate change, desertification, land degradation, sustainable land management, food security, and greenhouse gas fluxes in terrestrial ecosystems* (1st ed.). Cambridge University Press. <https://doi.org/10.1017/9781009157988>
- Jacobs, J. H., Viboud, C., Tchetchen, E. T., Schwartz, J., Steiner, C., Simonsen, L., & Lipsitch, M. (2014). The association of meningococcal disease with influenza in the United States, 1989–2009. *PLoS One*, 9(9), e107486. <https://doi.org/10.1371/journal.pone.0107486>
- Johnson, N. C., Xie, S.-P., Kosaka, Y., & Li, X. (2018). Increasing occurrence of cold and warm extremes during the recent global warming slowdown. *Nature Communications*, 9(1), 1724. <https://doi.org/10.1038/s41467-018-04040-y>
- Lowen, A. C., Mubareka, S., Steel, J., & Palese, P. (2007). Influenza virus transmission is dependent on relative humidity and temperature. *PLoS Pathogens*, 3(10), e151. <https://doi.org/10.1371/journal.ppat.0030151>
- Lowen, A. C., Steel, J., Mubareka, S., & Palese, P. (2008). High temperature (30°C) blocks aerosol but not contact transmission of influenza virus. *Journal of Virology*, 82(11), 5650–5652. <https://doi.org/10.1128/JVI.00325-08>
- Mackenzie, L. (2024). The burden of Influenza. Retrieved from <https://www.who.int/news-room/feature-stories/detail/the-burden-of-influenza>

- Mahmud, A. S., Martinez, P. P., & Baker, R. E. (2023). The impact of current and future climates on spatiotemporal dynamics of influenza in a tropical setting. *PNAS Nexus*, 2(9), pgad307. <https://doi.org/10.1093/pnasnexus/pgad307>
- Martinez, M. E. (2018). The calendar of epidemics: Seasonal cycles of infectious diseases. *PLoS Pathogens*, 14(11), e1007327. <https://doi.org/10.1371/journal.ppat.1007327>
- Mirsaedi, M., Motahari, H., Taghizadeh Khamesi, M., Sharifi, A., Campos, M., & Schraufnagel, D. E. (2016). Climate change and respiratory infections. *Annals of the American Thoracic Society*, 13(8), 1223–1230. <https://doi.org/10.1513/AnnalsATS.201511-729PS>
- National Research Council (US) Committee on Climate, E. (2001). Toward the Development of disease early warning systems. In *Under the weather: Climate, ecosystems, and infectious disease*. National Academies Press (US). Retrieved from <https://www.ncbi.nlm.nih.gov/books/NBK222241/>
- Osland, M. J., Stevens, P. W., Lamont, M. M., Brusca, R. C., Hart, K. M., Waddle, J. H., et al. (2021). Tropicalization of temperate ecosystems in North America: The northward range expansion of tropical organisms in response to warming winter temperatures. *Global Change Biology*, 27(13), 3009–3034. <https://doi.org/10.1111/gcb.15563>
- Paynter, S. (2015). Humidity and respiratory virus transmission in tropical and temperate settings. *Epidemiology and Infection*, 143(6), 1110–1118. <https://doi.org/10.1017/S0950268814002702>
- Pierce, D. (2023). ncd4: Interface to Unidata netCDF (version 4 or Earlier) format data files. Retrieved from <https://CRAN.R-project.org/package=ncdf4>
- Prosser, D. J., Teitelbaum, C. S., Yin, S., Hill, N. J., & Xiao, X. (2023). Climate change impacts on bird migration and highly pathogenic avian influenza. *Nature Microbiology*, 8(12), 2223–2225. <https://doi.org/10.1038/s41564-023-01538-0>
- Python Software Foundation. (2024). Python Language Reference, version 3.12.3 (Version 3.12.3) [Computer software]. Retrieved from <http://www.python.org>
- R Core Team. (2024). *R: A language and environment for statistical computing*. R Foundation for Statistical Computing. Retrieved from <https://www.R-project.org/>
- Shaman, J., & Kohn, M. (2009). Absolute humidity modulates influenza survival, transmission, and seasonality. *Proceedings of the National Academy of Sciences of the United States of America*, 106(9), 3243–3248. <https://doi.org/10.1073/pnas.0806852106>
- Shaman, J., Pitzer, V. E., Viboud, C., Grenfell, B. T., & Lipsitch, M. (2010). Absolute humidity and the seasonal onset of influenza in the continental United States. *PLoS Biology*, 8(2), e1000316. <https://doi.org/10.1371/journal.pbio.1000316>
- Soetaert, K., Petzoldt, T., & Woodrow Setzer, R. (2010). Solving Differential equations in R: Package deSolve. *Journal of Statistical Software*, 33(9), 1–25. <https://doi.org/10.18637/jss.v033.i09>
- Tamerius, J., Nelson, M. I., Zhou, S. Z., Viboud, C., Miller, M. A., & Alonso, W. J. (2011). Global influenza seasonality: Reconciling patterns across temperate and tropical regions. *Environmental Health Perspectives*, 119(4), 439–445. <https://doi.org/10.1289/ehp.1002383>
- Tamerius, J. D., Shaman, J., Alonso, W. J., Bloom-Feshbach, K., Uejio, C. K., Comrie, A., & Viboud, C. (2013). Environmental predictors of seasonal influenza epidemics across temperate and tropical climates. *PLoS Pathogens*, 9(3), e1003194. <https://doi.org/10.1371/journal.ppat.1003194>
- Viboud, C., Alonso, W. J., & Simonsen, L. (2006). Influenza in tropical regions. *PLoS Medicine*, 3(4), e89. <https://doi.org/10.1371/journal.pmed.0030089>
- Viboud, C., Bjørnstad, O. N., Smith, D. L., Simonsen, L., Miller, M. A., & Grenfell, B. T. (2006). Synchrony, waves, and spatial hierarchies in the spread of influenza. *Science (New York, N.Y.)*, 312(5772), 447–451. <https://doi.org/10.1126/science.1125237>
- Wickham, H. (2007). Reshaping data with the reshape Package. *Journal of Statistical Software*, 21(12), 1–20. <https://doi.org/10.18637/jss.v021.i12>
- Wickham, H., Averick, M., Bryan, J., Chang, W., McGowan, L. D., François, R., et al. (2019). Welcome to the tidyverse. *Journal of Open Source Software*, 4(43), 1686. <https://doi.org/10.21105/joss.01686>
- Yuan, H., Kramer, S. C., Lau, E. H. Y., Cowling, B. J., & Yang, W. (2021). Modeling influenza seasonality in the tropics and subtropics. *PLoS Computational Biology*, 17(6), e1009050. <https://doi.org/10.1371/journal.pcbi.1009050>